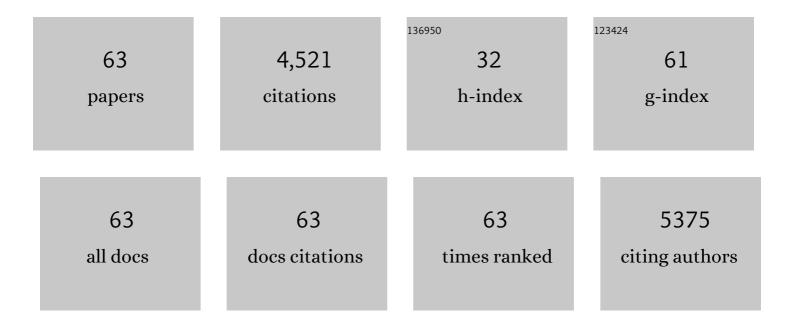
Young-Sang Yu

List of Publications by Year in descending order

Source: https://exaly.com/author-pdf/2655898/publications.pdf Version: 2024-02-01



#	Article	IF	CITATIONS
1	Chemical composition mapping with nanometre resolution by soft X-ray microscopy. Nature Photonics, 2014, 8, 765-769.	31.4	371
2	Origin and hysteresis of lithium compositional spatiodynamics within battery primary particles. Science, 2016, 353, 566-571.	12.6	367
3	Intergranular Cracking as a Major Cause of Long-Term Capacity Fading of Layered Cathodes. Nano Letters, 2017, 17, 3452-3457.	9.1	361
4	Correlative operando microscopy of oxygen evolution electrocatalysts. Nature, 2021, 593, 67-73.	27.8	321
5	The Formation Mechanism of Fluorescent Metal Complexes at the Li _{<i>x</i>} Ni _{0.5} Mn _{1.5} O _{4â^î^} /Carbonate Ester Electrolyte Interface. Journal of the American Chemical Society, 2015, 137, 3533-3539.	13.7	182
6	Direct Observation of Reversible Magnesium Ion Intercalation into a Spinel Oxide Host. Advanced Materials, 2015, 27, 3377-3384.	21.0	178
7	Quantification of Heterogeneous Degradation in Liâ€Ion Batteries. Advanced Energy Materials, 2019, 9, 1900674.	19.5	176
8	A highly stabilized Ni-rich NCA cathode for high-energy lithium-ion batteries. Materials Today, 2020, 36, 73-82.	14.2	163
9	Reliable low-power control of ultrafast vortex-core switching with the selectivity in an array of vortex states by in-plane circular-rotational magnetic fields and spin-polarized currents. Applied Physics Letters, 2008, 92, .	3.3	159
10	Unlocking anionic redox activity in O3-type sodium 3d layered oxides via Li substitution. Nature Materials, 2021, 20, 353-361.	27.5	155
11	A tailored oxide interface creates dense Pt single-atom catalysts with high catalytic activity. Energy and Environmental Science, 2020, 13, 1231-1239.	30.8	140
12	Three-dimensional localization of nanoscale battery reactions using soft X-ray tomography. Nature Communications, 2018, 9, 921.	12.8	107
13	Persistent and partially mobile oxygen vacancies in Li-rich layered oxides. Nature Energy, 2021, 6, 642-652.	39.5	106
14	Universal Criterion and Phase Diagram for Switching a Magnetic Vortex Core in Soft Magnetic Nanodots. Physical Review Letters, 2008, 101, 267206.	7.8	104
15	Fluid-enhanced surface diffusion controls intraparticle phase transformations. Nature Materials, 2018, 17, 915-922.	27.5	104
16	The chemistry and structure of calcium (alumino) silicate hydrate: A study by XANES, ptychographic imaging, and wide- and small-angle scattering. Cement and Concrete Research, 2019, 115, 367-378.	11.0	104
17	Fictitious phase separation in Li layered oxides driven by electro-autocatalysis. Nature Materials, 2021, 20, 991-999.	27.5	101
18	Dependence on Crystal Size of the Nanoscale Chemical Phase Distribution and Fracture in Li _{<i>x</i>} FePO ₄ . Nano Letters, 2015, 15, 4282-4288.	9.1	99

#	Article	IF	CITATIONS
19	Logic Operations Based on Magnetic-Vortex-State Networks. ACS Nano, 2012, 6, 3712-3717.	14.6	84
20	Cation ordered Ni-rich layered cathode for ultra-long battery life. Energy and Environmental Science, 2021, 14, 1573-1583.	30.8	83
21	Visualization of electrochemically driven solid-state phase transformations using operando hard X-ray spectro-imaging. Nature Communications, 2015, 6, 6883.	12.8	80
22	Synchrotron X-ray nanotomographic and spectromicroscopic study of the tricalcium aluminate hydration in the presence of gypsum. Cement and Concrete Research, 2018, 111, 130-137.	11.0	79
23	Intercalation of Magnesium into a Layered Vanadium Oxide with High Capacity. ACS Energy Letters, 2019, 4, 1528-1534.	17.4	75
24	Memory-bit selection and recording by rotating fields in vortex-core cross-point architecture. Applied Physics Letters, 2011, 98, .	3.3	60
25	Observation of coupled vortex gyrations by 70-ps-time- and 20-nm-space-resolved full-field magnetic transmission soft x-ray microscopy. Applied Physics Letters, 2010, 97, .	3.3	47
26	An ultrahigh-resolution soft x-ray microscope for quantitative analysis of chemically heterogeneous nanomaterials. Science Advances, 2020, 6, .	10.3	47
27	Nanometer-Resolved Spectroscopic Study Reveals the Conversion Mechanism of CaOA·Al ₂ O ₃ A·10H _{O to 2CaOA·Al₂O₃A·8H₂O and 3CaOA·Al₂O₃A·6H₂O at an Elevated Temperature. Crystal Growth}	3.0	44
28	Nonequilibrium Pathways during Electrochemical Phase Transformations in Single Crystals Revealed by Dynamic Chemical Imaging at Nanoscale Resolution. Advanced Energy Materials, 2015, 5, 1402040.	19.5	42
29	The Hydration of β- and α′ _H -Dicalcium Silicates: An X-ray Spectromicroscopic Study. ACS Sustainable Chemistry and Engineering, 2019, 7, 2316-2326.	6.7	42
30	Out-of-plane current controlled switching of the fourfold degenerate state of a magnetic vortex in soft magnetic nanodots. Applied Physics Letters, 2010, 96, 072507.	3.3	39
31	Near-edge X-ray refraction fine structure microscopy. Applied Physics Letters, 2017, 110, .	3.3	39
32	Dynamics of the Bloch point in an asymmetric permalloy disk. Nature Communications, 2019, 10, 593.	12.8	33
33	Removal of Hexavalent Chromium in Portland Cement Using Ground Granulated Blast-Furnace Slag Powder. Materials, 2018, 11, 11.	2.9	31
34	Understanding eigenfrequency shifts observed in vortex gyrotropic motions in a magnetic nanodot driven by spin-polarized out-of-plane dc current. Applied Physics Letters, 2008, 93, .	3.3	30
35	Vortex–antivortex pair driven magnetization dynamics studied by micromagnetic simulations. Applied Physics Letters, 2004, 85, 1568-1570.	3.3	29
36	Nanoscale Detection of Intermediate Solid Solutions in Equilibrated Li _{<i>x</i>} FePO ₄ Microcrystals. Nano Letters, 2017, 17, 7364-7371.	9.1	27

#	Article	IF	CITATIONS
37	Correlative image learning of chemo-mechanics in phase-transforming solids. Nature Materials, 2022, 21, 547-554.	27.5	27
38	Multivalent Electrochemistry of Spinel Mg _{<i>x</i>} Mn _{3–<i>x</i>} O ₄ Nanocrystals. Chemistry of Materials, 2018, 30, 1496-1504.	6.7	23
39	Automatic projection image registration for nanoscale X-ray tomographic reconstruction. Journal of Synchrotron Radiation, 2018, 25, 1819-1826.	2.4	23
40	Probing the Location and Speciation of Elements in Zeolites with Correlated Atom Probe Tomography and Scanning Transmission Xâ€Ray Microscopy. ChemCatChem, 2019, 11, 488-494.	3.7	19
41	Simultaneous control of magnetic topologies for reconfigurable vortex arrays. NPG Asia Materials, 2017, 9, e348-e348.	7.9	18
42	Advanced denoising for X-ray ptychography. Optics Express, 2019, 27, 10395.	3.4	18
43	Multimodal x-ray and electron microscopy of the Allende meteorite. Science Advances, 2019, 5, eaax3009.	10.3	17
44	Low-Power Selective Control of Ultrafast Vortex-Core Switching by Circularly Rotating Magnetic Fields: Circular–Rotational Eigenmodes. IEEE Transactions on Magnetics, 2008, 44, 3071-3074.	2.1	15
45	Ptychographic Imaging of Nano-Materials at the Advanced Light Source with the Nanosurveyor Instrument. Journal of Physics: Conference Series, 2017, 849, 012028.	0.4	15
46	Robust X-Ray Phase Ptycho-Tomography. IEEE Signal Processing Letters, 2016, 23, 944-948.	3.6	14
47	4D Imaging of ZnO-Coated Nanoporous Al ₂ O ₃ Aerogels by Chemically Sensitive Ptychographic Tomography: Implications for Designer Catalysts. ACS Applied Nano Materials, 2021, 4, 621-632.	5.0	14
48	Oppositely rotating eigenmodes of spin-polarized current-driven vortex gyrotropic motions in elliptical nanodots. Applied Physics Letters, 2008, 92, .	3.3	13
49	Polarization-selective vortex-core switching by tailored orthogonal Gaussian-pulse currents. Physical Review B, 2011, 83, .	3.2	13
50	Resonant amplification of vortex-core oscillations by coherent magnetic-field pulses. Scientific Reports, 2013, 3, 1301.	3.3	13
51	Reversible Room-Temperature Fluoride-Ion Insertion in a Tunnel-Structured Transition Metal Oxide Host. ACS Energy Letters, 2020, 5, 2520-2526.	17.4	13
52	The COSMIC Imaging Beamline at the Advanced Light Source: a new facility for spectro-microscopy of nano-materials. Microscopy and Microanalysis, 2018, 24, 8-11.	0.4	12
53	Visualization of the Phase Propagation within Carbon-Free Li4Ti5O12 Battery Electrodes. Journal of Physical Chemistry C, 2016, 120, 29030-29038.	3.1	10
54	Topology-dependent stability of vortex-antivortex structures. Applied Physics Letters, 2021, 118, .	3.3	8

#	Article	IF	CITATIONS
55	An interface-proximity model for switchable interfacial uncompensated antiferromagnetic spins and their role in exchange bias. Applied Physics Letters, 2005, 86, 192512.	3.3	5
56	Mapping Competitive Reduction upon Charging in LiNi _{0.8} Co _{0.15} Al _{0.05} O ₂ Primary Particles. Chemistry of Materials, 2020, 32, 6161-6175.	6.7	5
57	Dataflow at the COSMIC Beamline - Stream Processing and Supercomputing. Microscopy and Microanalysis, 2018, 24, 58-59.	0.4	4
58	Correlative analysis of structure and chemistry of LixFePO4 platelets using 4D-STEM and X-ray ptychography. Materials Today, 2022, 52, 102-111.	14.2	4
59	Lessons learned from FeSb2O4 on stereoactive lone pairs as a design principle for anion insertion. Cell Reports Physical Science, 2021, 2, 100592.	5.6	3
60	Understanding Chemomechanical Li-ion Cathode Degradation through Multi-Scale, Multi-Modal X-ray Spectromicroscopy. Microscopy and Microanalysis, 2018, 24, 426-427.	0.4	2
61	Differential electron yield imaging with STXM. Ultramicroscopy, 2021, 222, 113198.	1.9	2
62	Soft x-ray linear dichroic ptychography: the study of crystal orientation in biominerals. , 2021, , .		2
63	Using Scanning Transmission X-ray Microscopy to Reveal the Origin of Lithium Compositional Spatiodynamics in Battery Materials. Microscopy and Microanalysis, 2017, 23, 888-889.	0.4	Ο